Am J Physiol Renal Physiol 293: F1489–F1500, 2007.
First published August 29, 2007; doi:10.1152/ajprenal.00256.2007.

A novel mechanism of renal blood flow autoregulation and the autoregulatory role of A_1 adenosine receptors in mice

Armin Just[1,2] and William J. Arendshorst[1,2,3]

[1]*Department of Cell and Molecular Physiology,* [2]*Carolina Cardiovascular Biology Center,* [3]*University of North Carolina Kidney Center, University of North Carolina at Chapel Hill, Chapel Hill, North Carolina*

Submitted 31 May 2007; accepted in final form 27 August 2007

Just A, Arendshorst WJ. A novel mechanism of renal blood flow autoregulation and the autoregulatory role of A_1 adenosine receptors in mice. *Am J Physiol Renal Physiol* 293: F1489–F1500, 2007. First published August 29, 2007; doi:10.1152/ajprenal.00256.2007.—Autoregulation of renal blood flow (RBF) is mediated by a fast myogenic response (MR; ~5 s), a slower tubuloglomerular feedback (TGF; ~25 s), and potentially additional mechanisms. A_1 adenosine receptors (A1AR) mediate TGF in superficial nephrons and contribute to overall autoregulation, but the impact on the other autoregulatory mechanisms is unknown. We studied dynamic autoregulatory responses of RBF to rapid step increases of renal artery pressure in mice. MR was estimated from autoregulation within the first 5 s, TGF from that at 5–25 s, and a third mechanism from 25–100 s. Genetic deficiency of A1AR (A1AR−/−) reduced autoregulation at 5–25 s by 50%, indicating a residual fourth mechanism resembling TGF kinetics but independent of A1AR. MR and third mechanism were unaltered in A1AR−/−. Autoregulation in A1AR−/− was faster at 5–25 than at 25–100 s suggesting two separate mechanisms. Furosemide in wild-type mice (WT) eliminated the third mechanism and enhanced MR, indicating TGF-MR interaction. In A1AR−/−, furosemide did not further impair autoregulation at 5–25 s, but eliminated the third mechanism and enhanced MR. The resulting time course was the same as during furosemide in WT, indicating that A1AR do not affect autoregulation during furosemide inhibition of TGF. We conclude that at least one novel mechanism complements MR and TGF in RBF autoregulation, that is slower than MR and TGF and sensitive to furosemide, but not mediated by A1AR. A fourth mechanism with kinetics similar to TGF but independent of A1AR and furosemide might also contribute. A1AR mediate classical TGF but not TGF-MR interaction.

renal hemodynamics; tubuloglomerular feedback; kidney myogenic response; afferent arteriole; macula densa

IT IS GENERALLY ACCEPTED that autoregulation of renal blood flow (RBF) is mediated by two mechanisms, the myogenic response (MR) and tubuloglomerular feedback (TGF) (2, 36, 39). The kinetics of these mechanisms have been well-characterized. Response times of MR in the whole kidney and in small vessels in situ are usually 10 s or less (7, 30, 55). This agrees with the finding that the upper frequency limit of autoregulation in the kidney is at ~0.1–0.2 Hz, which corresponds to a response time of 4–8 s to reach 99% completion assuming an ideal exponential time course (9, 11, 16, 20). TGF, in contrast, is substantially slower. Micropuncture studies demonstrate an initial delay of ~10 s and an overall response time for completion of 30–60 s that includes the delay (3, 10). Micropuncture (15, 28) and whole animal RBF studies show oscillations of TGF at ~0.033 Hz, suggesting a response time of ~30 s (9, 11, 16).

A few previous studies of RBF autoregulation indicate the participation of additional mechanisms with characteristics distinct from classical features of MR and TGF. In particular, a slow third regulatory component has been described with a time course of ~2 min and thus substantially slower than both MR and TGF (20, 21, 50, 57). A similar slow component has also been observed at a hypotensive level of renal arterial pressure (RAP) (8). Furthermore, components of autoregulation are observed that are slower than MR and resistant to TGF inhibition by furosemide (20–22, 57). However, a difference is noted in the kinetics of the furosemide-resistant component, being either similar to the slow third mechanism (57), similar to the kinetics of TGF (20, 21), or showing an intermediate response time (22). It is thus unclear whether the slow and the furosemide-resistant components of autoregulation reflect two separate entities or the same mechanism with variable kinetics. Furthermore, the possibility remains that the furosemide-resistant component is due to remnant or decelerated TGF rather than a separate mechanism, although doubling of the dose of furosemide yielded similar results and no further increase in diuresis (20). Also consistent with maximum inhibition of TGF are urinary concentrations of the diuretic in a range compatible with effective concentrations at the macula densa (24). Clarification of these issues has been hindered by the difficulty of experimentally manipulating TGF in vivo.

An essential component in the signaling cascade of TGF is the A_1 adenosine receptor (A1AR) on the smooth muscle cells of afferent arterioles (4, 43, 47, 52, 53). Two independent strains of A1AR-deficient mice are devoid of TGF in superficial cortical nephrons (4, 52). These animals thus provide a new approach to assess the functional role of TGF by interfering with a downstream effector segment of the signaling cascade as opposed to pharmacological inhibition by furosemide acting on the sensor component of TGF. We therefore employed a combination of these genetic and pharmacological tools to clarify the identity and characteristics of the additional mechanisms in RBF autoregulation.

Despite the known involvement of A1AR in the signaling cascade of TGF, evidence suggests transmission of TGF via P2X1 purinoreceptors (P2X1R) without involvement of A1AR (18, 31, 35, 40) (reviewed in Ref. 17). Support for A1AR is predominantly based on micropuncture studies of superficial cortical nephrons, whereas support for involvement of P2X1R mainly depends on autoregulatory responses of juxtamedullary

Address for reprint requests and other correspondence: A. Just, Dept. of Cell and Molecular Physiology, 6341 Medical Biomolecular Research Bldg., CB#7545, School of Medicine, Univ. of North Carolina at Chapel Hill, Chapel Hill, NC 27599-7545 (e-mail: just@med.unc.edu).

The costs of publication of this article were defrayed in part by the payment of page charges. The article must therefore be hereby marked "*advertisement*" in accordance with 18 U.S.C. Section 1734 solely to indicate this fact.

nephrons. The question therefore remains whether A1AR mediate TGF in all nephrons or only in a subpopulation and may thus provide for only a fraction of whole kidney TGF. Clarification and quantification of these questions require assessment of TGF at the whole kidney level. Although a recent study showed impaired autoregulation of RBF and glomerular filtration rate (GFR) in A1AR-deficient mice (14), a role of these receptors in non-TGF autoregulatory mechanisms is not known. To this end, we quantified the impact of A1AR on autoregulation, specifically on the autoregulatory components provided by TGF and other mechanisms.

Previous studies demonstrated an interaction between TGF and MR from micropuncture studies (45), from mathematical analysis of proximal tubular pressures (51) and RBF (42), and from the dynamics of diameter changes of juxtamedullary afferent arterioles in situ (55), as well as from the dynamics of RBF responses of the kidney in vivo (20, 22). Similar predictions have been made from model calculations (32, 37). Considering the importance of A1AR in mediating classical TGF, it is reasonable to postulate that interactions with MR are mediated by the same pathway. This assumption, however, has never been tested.

The present study had three aims: *1*) to study the existence of TGF-independent slow autoregulatory mechanisms in RBF autoregulation and to examine whether these mechanisms are identical or distinct when TGF deficiency results from the absence of A1AR or furosemide administration; *2*) to determine whether A1AR provide all or part of the composite TGF activity of the whole kidney; and *3*) to test whether interactions between TGF and MR are mediated by A1AR. To separate the autoregulatory mechanisms and their kinetics and thus allow quantification of their individual regulatory contributions, we analyzed the time course of autoregulation to a rapid step change in RAP. To take full advantage of both genetic and pharmacological approaches, we combined both targeted deletion of A1AR and furosemide for inhibition of TGF.

METHODS

Experiments were conducted on 16 gene-targeted mice deficient for A1AR [age 14–68 wk, body wt 24 ± 1 (20–45) g, left kidney weight 0.20 ± 0.02 (0.14–0.35) g, 10 males + 6 females] and 11 wild-type controls of the C57BL6 strain from the same colony [12–67 wk, 28 ± 2 (19–33) g, left kidney 0.23 ± 0.02 (0.13–0.29) g, 5 males + 6 females]. All animals were generously provided and genotyped by Dr. J. B. Schnermann [National Institutes of Health (NIH)-National Institute of Diabetes and Digestive and Kidney Diseases (NIDDK), Bethesda, MD] (52). Wild-type and null mutants were derived from heterozygous breeder pairs that had a mixed C57BL6/129J genetic background. Genotyped mice were transferred to North Carolina in three shipments in 2004/2005. At least 10 days were allowed for equilibration after relocation to Chapel Hill before experiments were begun. All experiments were conducted at the University of North Carolina at Chapel Hill in accordance with the Guide for the Care and Use of Research Animals and approved by the local Institutional Animal Care and Use Committee. Animals were fed a standard lab chow with free access to tap water and were kept on a 12:12-h light-dark cycle. Surgery and experimental procedures were similar to those reported previously for rats (20, 21).

Surgical Procedures

After induction of anesthesia by pentobarbital sodium (80 mg/kg, Nembutal, Abbott, Chicago, IL), the animals were placed on a temperature-controlled table kept at 37°C. The depth of anesthesia was monitored by the response to ear and toe pinching. Additional doses of pentobarbital sodium (3–10 mg/kg sc) were given as needed (every ~30–60 min). The left femoral artery was catheterized (PE-50 with tapered polyurethane tip) (33) to measure arterial pressure, and two catheters (tapered PE-10) were placed into the left femoral vein. An isoncotic bovine serum albumin solution was infused throughout the experiment (2.38 g/dl, 10 μl/min). The trachea was cannulated (PE-60) to facilitate respiration. Via a small suprapubic incision, the urinary bladder was exteriorized, emptied by a 27-gauge needle, and catheterized by a PE-10 catheter for drainage of urine by gravity. The mouse was then turned on its right side. Through a flank incision, the left kidney was approached retroperitoneally and the renal artery and adjacent aorta were exposed. A custom-built mechanical occluder was placed on the aorta as far cranially as possible, usually above the superior mesenteric artery, to minimize mechanical impact on the flow measurement. A flow probe [0.5 PSB (in 11 knockout and 8 wild-type mice) or 0.5 VB (5 and 3 mice)] was implanted on the left renal artery and filled with coupling gel. No apparent differences were observed between results obtained with either probe. Baseline blood flow was identical with both probes implanted sequentially in one animal.

Sixty minutes were allowed for stabilization after surgery. Pressure in the left renal artery (RAP) was measured via the femoral artery catheter and a pressure transducer (Statham P23B). RBF was measured by the flow probe connected to an ultrasound transit-time flowmeter (TS-420, Transonic, low-pass filter 30–40 Hz). Zero offset was determined at the end of each experiment after cardiac arrest. A footswitch was used to produce a 1-V signal for indication of the time points of induction and release of the pressure reduction. All data were recorded on a computer at 100 Hz (RAP and RBF) or 10 Hz (footswitch signal). Urinary flow was measured repeatedly using a graduated cylinder.

The autoregulatory response of RBF to a rapid change of RAP within the autoregulatory pressure range was measured after RAP was reduced by 20 mmHg by partial occlusion of the aorta. RAP reduction was attained through manual control of the screw-actuator of the implanted occluder according to measured RAP. RAP was reduced for a period of 60 s similar to previous methodology using a pneumatic balloon occluder in rats (20, 21). A 20-mmHg step increase in RAP was then produced by rapid release of the occlusion. RAP reductions were repeated every 5 min, thus allowing 4 min for recovery. At least three RAP steps were made in each period. At the conclusion of the experiments, the animals were euthanized by an overdose of pentobarbital sodium (>200 mg/kg sc and ip).

Experimental Protocols

Genetic absence of A1AR (wild-type: n = 11, 5 males/6 females; knockout: n = 16, 10 males/6 females). To investigate the effect of elimination of TGF by genetic means, autoregulatory responses to pressure steps were compared between wild-type and A1AR-deficient mice. Multiple responses were recorded in each animal (9 ± 1 in wild-type, 9 ± 1 in knockout). Genotyping was done at NIH-NIDDK as described previously (52). For phenotypic confirmation, cardiac and renovascular responses to injection of the A1AR agonist cyclohexyl-adenosine (CHA; 0.5–1 μg in 25–50 μl saline iv) were measured at the end of an experiment in 7 wild-type and 10 A1AR-deficient animals.

Effect of furosemide in the absence of A1AR (wild-type: n = 6, 4 males/2 females; knockout: n = 8, 6 males/2 females, subgroup from above). To assess whether A1AR-deficient mice retain a remnant TGF activity contributing to RBF autoregulation, step responses were also investigated during TGF inhibition by furosemide (10 mg/kg iv in 1 ml/kg saline) given after the control period. Fifteen minutes were allowed for equilibration after furosemide injection. For comparison and to ensure that furosemide has a comparable effect in normal mice as in rats, the same experiment was also conducted in wild-type mice.

Three to six step responses were recorded during furosemide in each mouse. To replace fluid loss, the albumin solution was diluted 10-fold with saline and infused at 100 μl/min. Voided urine and infused volume were compared every 5 min and the infusion rate was adjusted as necessary to keep the volume balance between 0 and at most +1 ml.

Data Analysis

The 100-Hz data of RAP and RBF were smoothed by a sliding average over 50 values each. Renal vascular resistance (RVR) was calculated as renal perfusion pressure (RPP)/RBF, where RPP = RAP − 4 mmHg; 4 mmHg was assumed as renal venous pressure. These data sets of RAP, RBF, and RVR were then decimated to a sampling rate of 10 Hz. Short segments were extracted into single files for each RAP reduction containing the last 10 s before RAP reduction, followed by the segment between the last 10 s before release through 120 s after release. For analysis of the responses to a RAP decrease, segments were extracted containing the data from 10 s before RAP reduction through the time of RAP release. The exact time points for release of RAP were derived from the footswitch signal. Because the occluder is kept more open than the resting aortic diameter, beginning of aortic constriction is not immediate; time points for the reduction of RAP were therefore roughly estimated from the footswitch signal and subsequently determined more exactly from inspection of the individual RAP tracing. Baseline values given in Table 1 are the mean values during the 10 s before each RAP reduction during a particular experimental period. First and second derivatives of RVR were calculated from the time courses of RVR by applying the Savitzky-Golay algorithm with a window size of 11 points and coefficients for third-order fitting.

Autoregulatory efficiency was expressed as percent of perfect autoregulation, with 100% denoting a RVR adjustment matched to keep RBF constant in the face of a change in RAP; 0% indicates unchanged RVR and the absence of effective autoregulation. The efficiency of total RBF autoregulation was calculated as $(RVR_{end} - RVR_{pre})/[(RPP_{end}/RBF_{pre}) - RVR_{pre}] * 100$, where RPP_{pre}, RBF_{pre}, and RVR_{pre} are averages for the last 10 s before release of the aortic occluder, and RVR_{end} and RPP_{end} are the average values during 90–120 s after the step increase in RAP. The time course of RVR was normalized by the same formula substituting RVR_{end} by each individual RVR over time. The contribution of regulatory mechanisms was derived from the autoregulatory efficiency achieved by certain time points after the pressure step. The time points were chosen based on a three-component linear regression model of the RVR time course, which indicated transition times between components at 4.4 and 23.0 s. In addition, as in previous studies (20, 21), the transition between the first (MR) and the secondary response (TGF) was also determined from the time of lowest speed of RVR change within the first 10 s after the RAP step. This was derived from the second derivative of RVR. The exact time of zero crossing of the second derivative was determined from the individual time courses during control conditions of each animal by calculating a linear regression over the derivative between 3 and 9 s and finding the zero crossing of the regression line. Autoregulatory efficiency of each mechanism was estimated from the improvement in autoregulation from one time point to the next. To reduce scatter, the designated time points were represented by averages over ranges of time. Thus autoregulation provided by MR was estimated from the change in autoregulation achieved from the smallest RVR at 0–1 s to the level at 4–7 s after the pressure step. The change in autoregulation from 4–7 to 20–30 s was used for the contribution of TGF and/or fourth mechanism. The final improvement of autoregulation from 20–30 to 90–120 s was ascribed to the third mechanism.

Table 1. *Baseline hemodynamic data*

Group	RAP, mmHg	RBF, ml·min^{-1}·g KW^{-1}	*N*
Wild type	99±1	7.9±0.5	11 (5+6)
A1AR−/−	102±3	8.0±0.7	16 (10+6)
Wild-type control	99±2	8.0±0.6	5 (2+3)
Wild-type furosemide	100±3	7.9±0.8	5 (2+3)
A1AR−/− control	103±3	8.0±0.9	8 (6+2)
A1AR−/− furosemide	105±3	7.2±0.8*	8 (6+2)

Values are means ± SE. RAP, mean arterial pressure; RBF, renal blood flow; A1AR, A_1 adenosine receptor; KW, kidney weight; *N*, number of animals (males + females). *$P < 0.05$ vs. respective wild-type.

Likewise, autoregulatory efficiency for the response to step reduction RAP was calculated by taking for RPP_{pre}, RBF_{pre}, and RVR_{pre} the averages for the last 10 s before RAP reduction, and for RVR_{end} and RPP_{end} the average values during 50–60 s after RAP reduction. Time points for the initial passive resistance change as well as for the actions of MR and TGF/fourth mechanism were the same as those used during analysis of step increases of RAP (0–1, 4–7, and 20–30 s, respectively).

To determine the speed of the autoregulatory mechanisms, the slopes of linear regression lines were determined in three representative time windows from the time course of normalized RVR. Units are in percent of perfect autoregulation per second. The time windows were chosen from the best fit by a set of three consecutive linear regression lines within the time window of 0.5 to 100 s. To find the two optimum transition times between the three intervals, an iteractive procedure was applied to the averaged time course of all wild-type mice (Fig. 1*B*). Transition times between intervals were initially set to 10 and 30 s. Regression lines were calculated over these three subintervals and the intersection points were determined. The next iteration was calculated setting the new transition times to the intersection points of the previous iteration. The approximation was terminated when either intersection point varied by <0.2 s between iterations. This was the case after 12 iterations, giving intersection times of 4.4 and 23.0 s. For determination of individual slopes and intersections in each animal and each experimental condition, regression lines were then calculated from individual curves using fixed intervals transitioning at 5 and 25 s.

Statistical Analysis

Statistical significance was tested by ANOVA for repeated measures in conjunction with Holm-Sidak or Tukey's post hoc test according to recommendations of the software (SigmaStat 3.5, SPSS, Chicago, IL). In case of non-normal distribution, Tukey's test for multiple comparisons was used as a post hoc test. A P value <0.05 was considered statistically significant. Data are represented as means ± SE. Numbers of sample sizes (*n*) refer to the number of animals.

RESULTS

Baseline values of RAP and RBF are given in Table 1. Heart rates were 619 ± 33 beats/min in wild-type and 639 ± 19 beats/min in A1AR-deficient mice and did not differ among strains or experimental groups. Baseline urine flow was 3.6 ± 0.5 μl/min in wild-type mice and 5.1 ± 0.8 μl/min in A1AR-deficient mice ($P > 0.2$).

Control Autoregulatory Responses in Wild-Type Mice

Characteristics of autoregulation under basal conditions are summarized in the figures and in Tables 2-5. The left panels in each figure display the response to a ~20-mmHg step increase of RAP; the right panels give the response to a 20-mmHg step reduction of RAP. Figure 1, *top*, shows the time course of RAP, demonstrating a rapid sufficiently square-shaped change

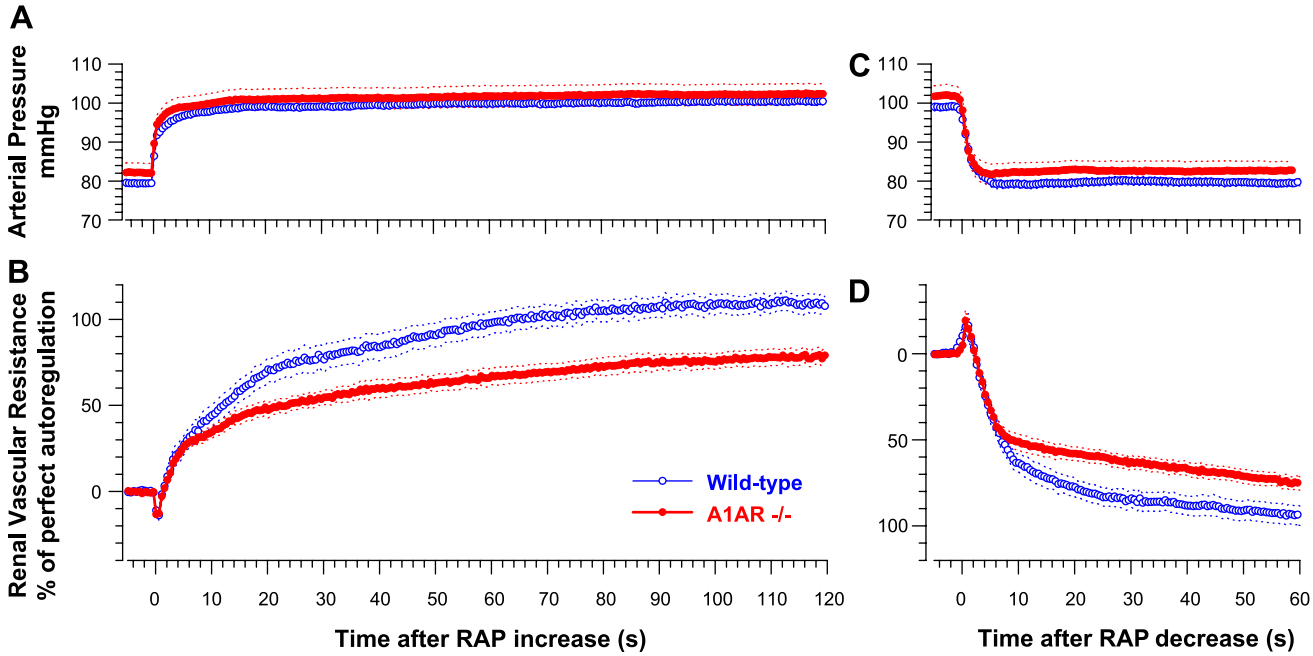

Fig. 1. Dynamics of renal blood flow autoregulation in the presence and absence of A_1 adenosine receptors (A1AR). Time course of the autoregulatory response of renal vascular resistance (RVR; *B* and *D*) to a 20-mmHg step increase (*B*) or decrease (*D*) of renal arterial pressure (RAP; *A* and *C*) in wild-type (○, $n = 11$) and A1AR-deficient mice (A1AR−/−, ●, $n = 16$). Means ± SE. Only every 10th data point is plotted for clarity.

in RAP. As reported previously for rats, the RVR response to an increase in RAP during control conditions in mice was characterized by the following features (○ in Fig. 1): after an initial drop, RVR rose quickly within the first 5–10 s. A secondary rise of RVR began at ~10 s and slowed down at ~20–30 s. Between ~30 and 120 s, RVR further increased in a third time course that was the slowest. Further support for the third time course is provided by improvement of autoregulation from 20–30 to 90–120 s after the pressure step (from 72 ± 8 to 104 ± 6%, $P < 0.001$) and positive linear correlation of RVR over time between 25 and $t = 100$ s ($P < 0.001$ in each animal), with an average slope greater than zero (Table 2, $P < 0.001$). From these response times and from previous studies (20, 21), the initial autoregulatory response within the first 10 s is considered to reflect MR, the secondary rise between 10 and 30 s TGF, and the slow response between 30 and 120 s a third regulatory mechanism.

To more rigorously determine the time intervals of the regulatory mechanisms, we approximated the time course of autoregulation by three linear regression lines, so that the first interval indicates MR, the second TGF, and the third interval the third mechanism. An iterative fitting performed on the average time course from all control experiments indicated the best approximation for interval transitions at 4.4 and 23.0 s in wild-type mice (Fig. 2). Individual intersection points were then calculated for each animal and experimental period using fixed regression intervals (0.5 to 5 s, 5 to 25 s, 25 to 100 s). This gave average intersection points of 4.9 and 23.1 s (Table 3). As another measure for the transition time between MR and TGF, the point of the

Table 2. *Strength of overall autoregulation and contributing autoregulatory effects of the underlying mechanisms in response to a step-increase of renal arterial pressure*

Group	Total Steady-State Autoregulation from Prestep to 90–120 s	Contributing Autoregulatory Effects			*N*
		Myogenic Response from 0–1 to 4–7 s	TGF and/or Fourth Mechanism from 4–7 to 20–30 s	Third Mechanism from 20–30 to 90–120 s	
		% of Perfect autoregulation			
Wild type	104±6	40±5	44±5	32±5	11
A1AR−/−	73±4[c]	37±3	23±3[b]	24±3	16
Wild-type control	90±7	35±6	38±1	33±9	5
Wild-type furosemide	85±8	62±4[e]	34±4	3±6[d]	5
A1AR−/− control	71±8[a]	34±3	19±4[a]	27±4	8
A1AR−/− furosemide	88±6	51±4[d]	34±5[d]	6±5[d]	8

Values are means ± SE. TGF, tubuloglomerular feedback. [a,b,c]:$P < 0.05$, $P < 0.01$, $P < 0.001$ vs. respective wild-type. [d,e]:$P < 0.05$, $P < 0.01$ vs. respective control. The sum of contributions exceeds 100% because the contribution of the myogenic response is calculated as beginning from the initial reduction of resistance after the pressure step. Total steady-state autoregulation, in contrast, is measured from the prestep level.

Table 3. *Results of the 3-component linear regression fitting of the autoregulatory response to a step-increase in renal artery pressure*

Group	Slopes of Regression Lines			Intersection Points		*N*
	Myogenic Response 0.5 to 5 s	TGF and/or Fourth Mech. 5 to 25 s	Third mechanism 25 to 100 s	Myogenic response 5 to 25 s	TGF 25 to 100 s	
	% of Perfect autoregulation/s					
Wild type	9±1	2.4±0.3	0.46±0.09[e]	4.9±0.3	23.1±2.1	11
A1AR−/−	8±1	1.3±0.2[b]	0.31±0.04[e]	4.9±0.2	22.6±2.8	16
Wild-type control	8±1	2.2±0.1	0.50±0.15[g]	4.7±0.4	24.1±2.3	5
Wild-type furosemide	13±1[d]	1.7±0.2	0.04±0.04[c,f,i]	5.0±0.2	23.8±1.0	5
A1AR−/− control	7±1	1.0±0.2[a]	0.36±0.06[f]	4.9±0.4	19.0±4.9	8
A1AR−/− furosemide	10±1	1.8±0.3	0.05±0.08[c,e,h]	5.4±0.4	23.8±1.2	8

Values are means ± SE. [a,b]:$P < 0.05$, $P < 0.001$ vs. respective wild-type. [c,d]:$P < 0.05$, $P < 0.01$ vs. respective control. [e,f,g]:$P < 0.05$, $P < 0.01$, $P < 0.001$ vs. TGF/Fourth Mechanism of the same group. [h]:not significantly different from 0.

slowest rise of RVR within the first 20 s was determined from the zero intercept of the second derivative of RVR, yielding 6 ± 1 s in wild-type mice.

Final steady-state autoregulation was 104% (Table 2), verifying that the small 20-mmHg pressure steps were within the autoregulatory pressure range. To determine the autoregulatory contributions of each mechanism, the change of autoregulation between designated time points was calculated. MR was represented by autoregulation from ~0.5 to ~5 s, TGF by that from ~5 to ~25 s, and the third regulatory mechanism in the time window of ~25 to ~100 s. In addition, a fourth regulatory mechanism seems to contribute to autoregulation in the same time window as TGF (20–22, and present study). Our results indicate that MR, TGF plus fourth mechanism, and third mechanism provide autoregulatory strengths of 40, 44, and 32%, respectively (Table 2). The sum of these contributions exceeds 100%, because the calculation for MR also includes the autoregulation required to restore RVR from its initial minimum back to baseline. Total steady-state autoregulation, in contrast, was calculated starting from the level preceding the step to indicate effective autoregulation and to facilitate comparisons with the literature. When these regulatory contributions are considered in relation to the total adaptation from the initial minimum to the final level (i.e., from 0–1 to 90–120 s), their relative participation was 35 ± 4, 37 ± 2, and 28 ± 5% of the observed overall response. Similar results were obtained when the degree of autoregulation was derived from autoregulation at the intersection points of the three-component linear regression model. This gave autoregulatory contributions of 37 ± 5, 47 ± 6, and 38 ± 7% of perfect autoregulation for MR (from $t = 0.5$ s to the first intersection point), TGF/fourth mechanism (from first to second intersection point), and third mechanism (from second intersection to $t = 100$ s). These values correspond to relative contributions of 31 ± 4, 39 ± 4, and 31 ± 6% of the overall autoregulatory response. The speed of the autoregulatory mechanisms, as determined from the slopes of the three regression lines were 9, 3, and 0.5%/s for MR, TGF/fourth mechanism, and third mechanism (Table 3).

Autoregulatory responses to step reduction of RAP were reciprocal, but otherwise similar to those reported for the step increase in RAP (Fig. 1*D*, Tables 4 and 5). A notable difference is that MR provided a larger degree of autoregulation to step reduction of RAP (52%; Table 4) than during step increase (40%, $P < 0.05$; Table 2) and the third mechanism substantially less (10 vs. 32%, $P < 0.001$). Corresponding relative contributions of MR, TGF/fourth mechanism, and third mechanism were 49 ± 3, 42 ± 2, and 10 ± 2%. Similarly, the speed of MR was greater for vasodilation following step reduction of RAP than for vasoconstriction after step increase (13 vs. 9% s, $P < 0.001$; Tables 5 vs. 3). No differences were observed between male and female mice, so their data were pooled.

Table 4. *Strength of overall autoregulation and contributions of the autoregulatory mechanisms in response to a step-decrease of renal arterial pressure*

Group	Total Steady-state Autoregulation from Prestep to 90–120 s	Contributions			*N*
		Myogenic Response from 0–1 to 4–7 s	TGF and/or Fourth Mechanism from 4–7 to 20–30 s	Third Mechanism from 20–30 to 50–60 s	
		% of Perfect autoregulation			
Wild-type	92±6	52±5	44±4	10±2	11
A1AR−/−	72±4*	48±3	23±3†	13±2	16
Wild-type control	82±8	42±4	43±2	11±4	5
Wild-type furosemide	69±4	52±9	41±5	4±1	5
A1AR−/− control	66±6	47±5	20±5*	12±3	8
A1AR−/− furosemide	88±5‡	65±5‡	29±5	5±2	8

Values are means ± SE. *·†:$P < 0.05$, $P < 0.001$ vs. respective wild-type. ‡:$P < 0.05$ vs. respective control. The sum of contributions exceeds 100% because the contribution of the myogenic response is calculated as beginning from the initial increase of resistance after the pressure step. Total steady-state autoregulation, in contrast, is measured from the prestep level.

Table 5. *Results of the 3-component linear regression fitting of the autoregulatory response to a step-decrease in renal artery pressure*

Group	Slopes of Regression Lines			Intersection Points		*N*
	Myogenic Response 0.5 to 5 s	TGF and/or Fourth Mech. 5 to 25 s	Third Mechanism 25 to 60 s	Myogenic response 5 to 25 s	TGF 25 to 100 s	
	% of Perfect autoregulation/s					
Wild-type	−13±1	−1.9±0.2	−0.33±0.07[e]	6.7±0.3	22.5±1.1	11
A1AR−/−	−12±1	−0.9±0.1[b]	−0.40±0.06[e]	1.3±0.3	25.8±7.2	16
Wild-type control	−11±2	−2.0±0.1	−0.39±0.13[e]	7.2±0.5	21.0±1.0	5
Wild-type furosemide	−13±2	−1.8±0.2	−0.11±0.03[e]	7.8±1.0	21.5±0.6	5
A1AR−/− control	−14±2	−0.9±0.27[a]	−0.40±0.09[e]	5.7±0.5	20.1±2.1	8
A1AR−/− furosemide	−17±2	−1.3±0.24	−0.10±0.06[e]	5.5±0.3	23.4±0.9	8

Values are means ± SE. [a,b]:$P < 0.05$, $P < 0.001$ vs. respective wild-type. [c,d,e]:$P < 0.05$, $P < 0.01$, $P < 0.001$ vs. TGF/Fourth Mechanism of the same group.

Autoregulation in the Absence of A1AR

Targeted deletion of A1AR, which is known to eliminate TGF (4, 52), led to impaired overall autoregulation (Fig. 1, *B* and *D*), as expected. Note that the loss of autoregulation was almost entirely due to attenuation of the secondary rise of RVR occurring in wild-type animals between 5 and 25 s after the step increase (Fig. 1*B*). This is reflected by the predominant loss of autoregulation in the time window ascribed to TGF and fourth mechanism (23 vs. 44%; Table 2), with only minor reductions in the contributions of MR (37 vs. 40%) and the third mechanism (24 vs. 32%). Similar results were obtained when autoregulatory contributions were calculated from the intersection points of the three-component linear model: autoregulatory strength in the time window of TGF and fourth mechanism was reduced from 47 ± 6 to 24 ± 4% ($P < 0.01$), while the contributions of MR (from 37 ± 5 to 35 ± 4%, $P > 0.8$) and of the third mechanism (38 ± 7 to 26 ± 3%, $P > 0.2$) were not affected. Likewise, the slope of the regression line in the TGF-related time window (5 to 25 s) was ~50% smaller in knockout animals than in wild-types, whereas slopes of MR and third mechanism did not significantly differ between strains (Fig. 2 and Table 3). The similarity of the kinetics of autoregulation between 25 and 100 s in wild-type and A1AR-deficient mice suggests the same underlying third mechanism in both strains.

It is surprising that the absence of A1AR did not abolish autoregulation in the time window assigned to TGF, instead reducing it by only ~50%. This remnant activity might reflect the action of the slower third mechanism starting before 25 s and/or remnant TGF activity, or yet another mechanism independent of classical TGF. Speaking against the third mechanism as the only explanation is the finding that the slope of autoregulation between 5 and 20 s was almost fivefold greater than that of the third mechanism (Table 3). Inspection of the time courses from individual animals indicated two subgroups (Fig. 3). Nine knockout animals displayed a monophasic rise of RVR after the initial MR, i.e., between 5 and 100 s, consistent with sole action of the third mechanism. The other seven mice showed a biphasic response with much faster regulation between 5 and 25 s than between 25 and 100 s, consistent with involvement of both third and fourth mechanisms. All animals with biphasic time course that were tested with the A1AR agonist CHA (4/7) were devoid of any vasoconstrictor or heart rate response to CHA, confirming the absence of A1AR. No relationship was found to gender (3 females in each subgroup), age (211 ± 44 vs. 258 ± 27 days), or RAP (103 ± 2 vs. 100 ± 6 mmHg). However, the subgroup with biphasic time course showed higher baseline RBF (9.1 ± 1.0 vs. 6.4 ± 0.6 $ml \cdot min^{-1} \cdot g^{-1}$, $P < 0.05$, 2.0 ± 0.4 vs. 1.7 ± 0.3 ml/min, $P > 0.4$). Further evidence for a biphasic pattern after MR comes from our iterative linear regression model applied to the average time course of all A1AR-deficient mice (Fig. 2); the approximation converged to a three-component model with transition points at similar times (4.9 and 25.5 s; Fig. 2) as in wild-type mice (4.4 and 23.0 s).

It is noteworthy that in contrast to the effect of TGF inhibition by furosemide (Fig. 4 and Table 2) (20, 21), the strength of MR was not affected by the genetic absence of

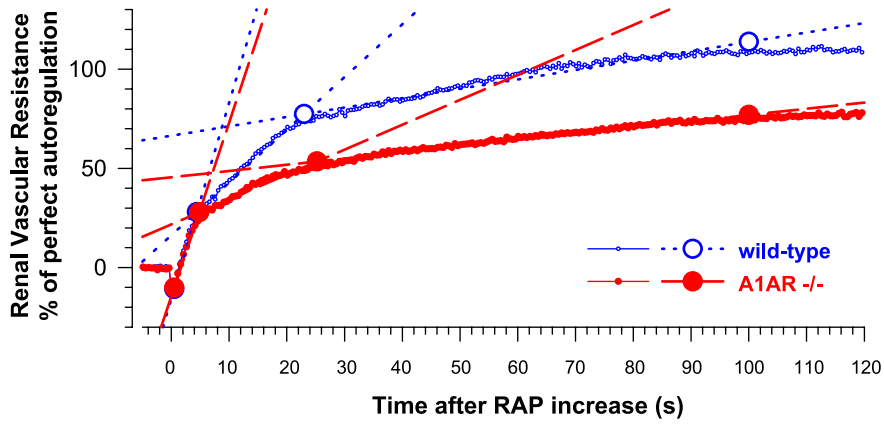

Fig. 2. Three-component linear regression model of the autoregulatory response in the presence and absence of A1AR. Time course of the autoregulatory response of RVR to a 20-mmHg step increase of RAP in wild-type (○, $n = 11$) and A1AR-deficient mice (A1AR−/−, ●, $n = 16$). Small symbols show group average of the experimental data (SE not shown for clarity). Large symbols and lines denote approximation by an iterative 3-component linear regression model (for details, see METHODS).

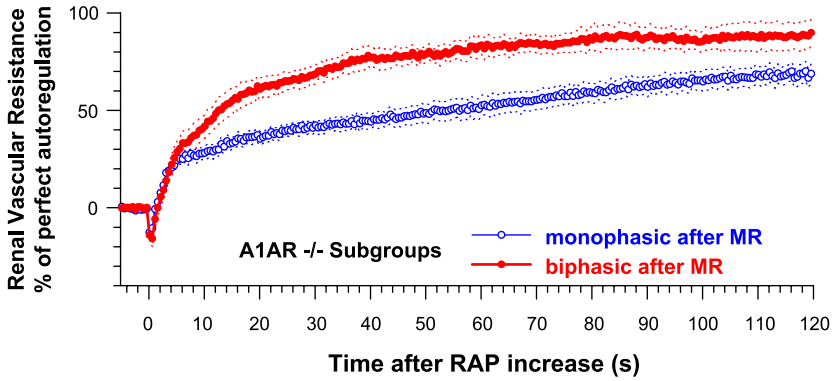

Fig. 3. Subgroup analysis of the autoregulatory response in A1AR-deficient mice. Time course of the autoregulatory response of RVR to a 20-mmHg step increase of RAP (*top*) in A1AR−/− (n = 16) separated into 2 subgroups: one subgroup with a rather uniform, monophasic rise of RVR between 5 and 120 s following the initial myogenic response (monophasic, ○, n = 9/16). Another group displayed a biphasic time course between 5 and 120 s with a more prominent RVR rise between 5 and 20 s than between 20 and 120 s (biphasic, ●, n = 7/16). Means ± SE.

A1AR (Fig. 1 and Table 2). This indicates that the previously described interaction between MR and TGF is not mediated nor modulated by the A1AR signaling pathway.

Similar results were observed in the autoregulatory response to step reduction of RAP (Fig. 1*D*, Tables 4 and 5). Overall autoregulation was depressed due to autoregulatory loss of TGF/fourth mechanism, with unaltered strengths of MR and third mechanism (Table 4). The speed of TGF/fourth mechanism was reduced, without effects on the kinetics of MR and third mechanism (Table 5). Nevertheless, even in the absence of A1AR, the speed of TGF/fourth mechanism remained significantly faster than that of the third mechanism (Table 5), compatible with two separate mechanisms.

The genotype of A1AR−/− animals was confirmed by absence of cardiac and renovascular responses to the A1AR agonist CHA (the online version of this article contains supplemental data). The response of heart rate (−46 ± 6% in wild-types, maximum at 20–40 s after injection) was completely abrogated (−2 ± 1%, $P < 0.01$ vs. wild-type), and the renal vasoconstrictor response to CHA (RBF reduced by 45 ± 4%, max. at 20–40 s) was converted into a small vasodilation (+8 ± 1%, max. at 40–60 s, $P < 0.001$ vs. wild-type and vs. 0).

Effect of Furosemide in Wild-Type Mice

To test whether the third regulatory mechanism is related to macula densa salt transport, the TGF-inhibiting agent furosemide was given to both wild-type and A1AR-deficient animals. Urine output increased 15- to 20-fold in wild-type (68 ± 11 vs. 3 ± 3 μl/min, $P < 0.001$) and knockout mice (63 ± 10 vs. 4 ± 1 μl/min, $P < 0.001$). Autoregulation in wild-type mice (Fig. 4*A*) was affected in a similar way as reported previously for rats (20, 21). *1*) The sluggish third mechanism was abolished (Table 2) and its corresponding slope depressed to a value not different from zero (Table 3). *2*) Substantial

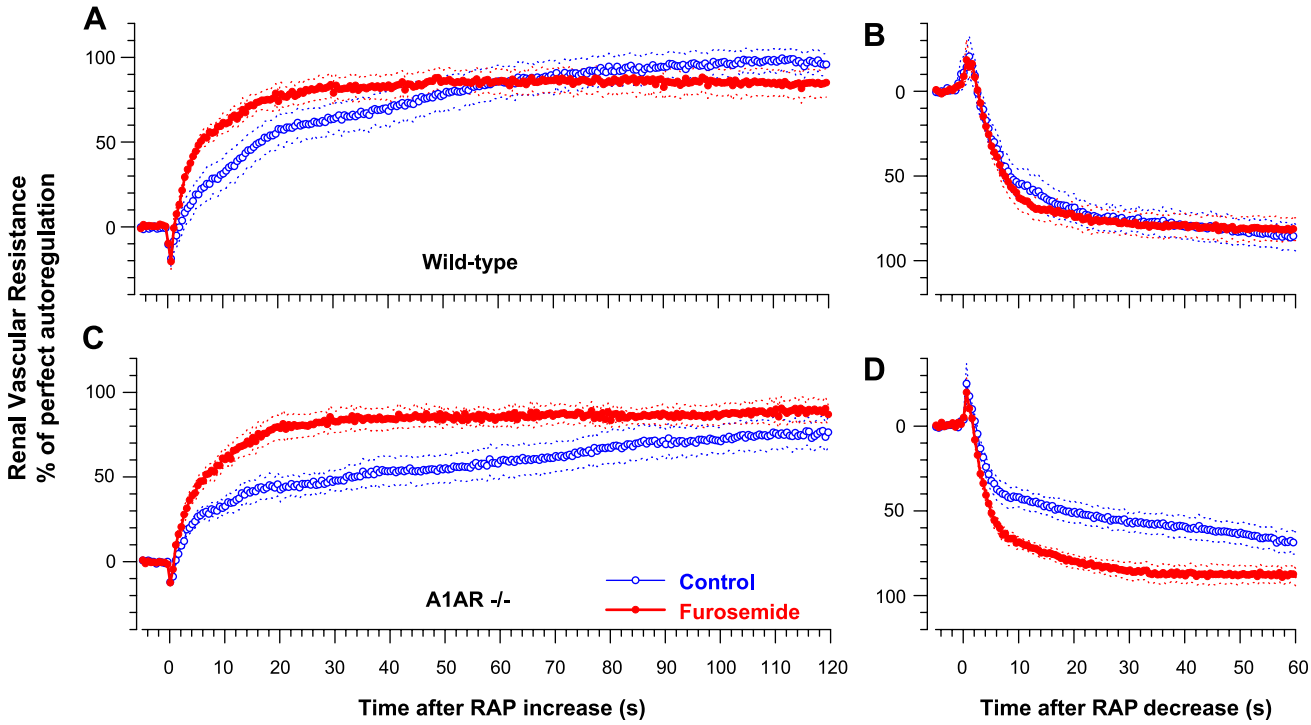

Fig. 4. Effect of furosemide on the dynamics of autoregulation in wild-type and A1AR−/− mice. Time course of the autoregulatory response of RVR to a 20-mmHg step increase (*A* and *C*) or decrease (*B* and *D*) of RAP during control conditions (○) and during TGF inhibition with furosemide (●). Data are presented for both wild-type mice (*A* and *B*, n = 5) and A1AR-deficient animals (*C* and *D*, n = 8). Means ± SE.

autoregulation remained in the intermediate time window of classical TGF (5 to 25 s, autoregulation improved from 27 ± 4 to 44 ± 7%, $P < 0.05$), with kinetics similar to those in the same time window during control conditions as evidenced by a similar slope (Table 3) and a similar intersection point with the third mechanism (Table 3). *3*) Both the strength (Table 2) and speed of MR (Table 3) were markedly enhanced. However, contrary to previous observations in rats (20, 21), autoregulation in the time window of classical TGF was not significantly reduced by furosemide (Table 2).

Effect of Furosemide in the Absence of A1AR

When furosemide was given to A1AR-deficient mice, the third mechanism was abolished and MR enhanced (Fig. 4, *C* and *D*, and Tables 2–5). In addition, a regulatory mechanism with kinetics similar to TGF was active between 5 and 25 s (Fig. 4), improving autoregulation from 49 ± 5 to 83 ± 6% ($P < 0.05$). This was the case without exception in all animals of this group, even those (6/8) which had displayed a "monophasic" time course before furosemide with no apparent difference to those with originally "biphasic" kinetics. Furthermore, the overall time course during furosemide was virtually identical to that during furosemide in wild-type mice, both quantitatively (MR: 51 vs. 62%, TGF/fourth: 34 vs. 34%, third: 6 vs. 3%, Table 2) and in its kinetics (MR: 10 vs. 13% s, TGF/fourth: 1.8 vs. 1.7% s, third: 0.05 vs. 0.04% s; Table 3). This agreement means that RBF autoregulation during furosemide, most notably the fourth mechanism, was not affected by the presence or absence of A1AR and thus unlikely mediated by these receptors. Furthermore, given the importance of A1AR for classical TGF, the finding also argues against incomplete inhibition of TGF as the explanation for this furosemide-resistant autoregulation. Note also that the strength of MR was enhanced by furosemide even in the absence of A1AR, which indicates that the known interaction between TGF and MR does not depend on this class of receptors. The subgroup of monophasic A1AR-deficient mice receiving furosemide responded similarly to the diuretic (Tables 2 and 3): MR was augmented from 32 ± 4 to 46 ± 3% ($P < 0.05$). Autoregulation in the time window of classical TGF and the putative fourth mechanism was smaller than in wild-type animals (15 ± 2%, $P < 0.05$). However, furosemide was found to enhance autoregulation in this time window to 31 ± 2% ($P < 0.001$), thereby reaching similar strength as during furosemide in wild-type mice (34%; Table 2). Likewise, furosemide increased the slope of the regression line between 25 and 30 s (0.7 ± 0.1 to 1.6 ± 0.1% s, $P < 0.001$), again resembling wild-types during furosemide (1.8% s; Table 3). Autoregulation provided by the third mechanism was 24 ± 4% before and 9 ± 7% during furosemide ($P > 0.1$).

Similar results were obtained in response to step reduction of RAP (Fig. 4, *B* and *D*, and Tables 4 and 5): Furosemide eliminated the third mechanism and enhanced MR at least in A1AR-deficient mice (Table 4) and did not or only partially reduced autoregulation in the time window of TGF and fourth mechanism.

DISCUSSION

The present study provides new information concerning the participation of at least one novel mechanism in RBF autoregulation in addition to traditional MR and classical TGF. This mechanism, which we refer to as the third autoregulatory mechanism, is substantially slower than classical TGF and independent of A1AR but is sensitive to furosemide. In addition, a putative fourth mechanism with kinetics similar to TGF, but independent of A1AR and apparently resistant to furosemide, may be involved. The relative participations of MR, TGF(+fourth), and third mechanism in the overall response are 35, 36(18+18), and 29% in wild-type mice. Classical TGF, indicated by furosemide-sensitive autoregulation between 5 and 25 s after the pressure step, is mediated completely by A1AR. In contrast, the known interaction between TGF and MR is independent of A1AR.

A1AR Mediate Classical TGF

Overall steady-state autoregulation was found to be impaired in A1AR-deficient animals, confirming the importance of TGF, as shown before (14). Our present results extend this finding by demonstrating that A1AR-dependent autoregulation is confined to the time window between 5 (4–7 s) and 25 s (20–30 s) normally seen in wild-type animals. Since A1AR-deficient mice are known to lack TGF, at least in superficial cortical nephrons, without other obvious abnormalities of renal function (4, 52), autoregulation in this time window most likely reflects classical TGF. This agrees with the known kinetics of classical TGF characterized by an initial lag period of ~10 s and an overall response time of 30–60 s (3, 10), as well as with spontaneous oscillations with a cycle length of 30 s (15, 28). Mice show similar TGF kinetics (52). Previous findings in rats indicate that furosemide reduces autoregulation in the time window of 5–25 s. Although furosemide did not have a similar effect in the present mouse study, it is conceivable that such an effect is masked by simultaneous augmentation of the contribution of another mechanism in the same time window. As discussed below, a fourth regulatory mechanism appears to operate at 5–25 s. As both previous data in rats (20, 21) and the present results in mice indicate an increased regulatory contribution of MR during furosemide, the fourth mechanism may be affected in a similar way. Consistent with this interpretation and the assumption of inhibited TGF contribution during furosemide is the observation that the absence of A1AR failed to further reduce autoregulation during furosemide.

Contribution of a Third Regulatory Mechanism

The autoregulatory response includes a third mechanism, one that is more sluggish than TGF and presents with a time course between 25 and 100 s (Figs. 1 and 2) as reported before in rats (20, 21, 50, 57). The present results demonstrate for mice the presence of a similar mechanism with virtually identical kinetics (Fig. 1). The substantially slower time course beyond 25 s suggests that it is distinct from both classical TGF and MR. Although the slow time course per se does not exclude that the third mechanism is caused by a slow modulation of the strength of TGF, our data strongly argue against this option. If it were due to an aspect of TGF, it should be sensitive to the elimination of A1AR. However, our data show that that strength and kinetics of the third mechanism are almost identical in wild-type and A1AR-deficient mice. Although independent of A1AR, the third mechanism was abolished by furosemide, suggesting that it shares with classical

TGF the dependence on Na^+-K^+-$2Cl^-$ cotransport or some function thereof.

Potential Contribution of a Fourth Regulatory Mechanism

When furosemide is given to wild-type animals, a remnant autoregulatory component is observed with a time course similar to that of classical TGF. The simplest explanation is that remnant TGF activity persists in the face of incomplete inhibition by furosemide. Although this cannot be entirely excluded, it seems unlikely, since the same time course, with regard to both strength and kinetics, was observed in A1AR-deficient animals during furosemide. If furosemide were inhibiting TGF only partially in all nephrons, then elimination of TGF by genetic deficiency of A1AR should have abolished this component of autoregulation. Even if TGF were dependent on A1AR only in some nephrons, the furosemide-resistant fourth component should have been attenuated by deficiency of A1AR. Otherwise, one would have to postulate that furosemide fails to affect TGF exclusively in those nephrons that do not depend on A1AR, which seems unlikely. Taken together, the data suggest that the fourth component of autoregulation is furosemide resistant rather than reflecting incompletely inhibited TGF. This furosemide-resistant mechanism could either be separate from the third mechanism, or it could represent the same mechanism but being accelerated by furosemide, e.g., due to enhanced tubular flow by the diuretic. In the latter case, however, the third and fourth component of autoregulation should not occur at the same time. Visual inspection of the average response in all A1AR-deficient mice suggests a biphasic time course indicative of fourth and third mechanism after MR, more clearly so in a subgroup of A1AR-deficient mice. The iterative linear regression model indicated two separate components in addition to the initial MR and converged to a transition point at 25.5 s, a time very similar to that found during furosemide in the presence (23.1 s) or absence of A1AR (20.3 s). Moreover, the model analysis using fixed regression intervals applied to the time course of each A1AR-deficient animal revealed different slopes ($P < 0.01$; Table 3) in the intervals of 5 to 25 and 25 to 100 s. It therefore seems more likely that the slowest and the furosemide-resistant component of autoregulation constitute two distinct mechanisms.

Collectively, our data indicate that at least one novel mechanism participates in RBF autoregulation in addition to MR and TGF. The third regulatory mechanism is slower than both MR and classical TGF, independent of A1AR, but sensitive to furosemide. In addition, a fourth mechanism exhibiting kinetics similar to classical TGF but independent of both A1AR and resistant to furosemide seems to contribute. Neither of these new mechanisms fits the characteristics of classical TGF. The underlying causes of these mechanisms await further investigation.

Potential Causes for the Third Regulatory Mechanism

An attractive candidate for the third mechanism is ATP acting on P2X1 receptors on the preglomerular vasculature. This signaling pathway has been reported to mediate TGF-like responses in juxtamedullary nephrons that were abolished by furosemide or papillectomy (17, 18). The response time might be longer in these deep cortical nephrons due to longer loops of Henle. Based on reported responses, kinetics appear to take up to 84 s for constriction and up to 132 s for the dilator response (18). The hypothesis that P2X1R mediate the sluggish third mechanism rather than classical TGF would also help to understand the conflicting findings concerning the importance of A1AR and P2X1R in macula densa signaling (17, 46).

Another possibility for the third mechanism is a TGF-like activity that appears to exist between the connecting tubule and afferent arteriole of superficial nephrons (38, 44). The slow response time might be explained by the longer travel time of the tubular fluid to the connecting tubule, and furosemide sensitivity might be caused by marked elevation of tubular NaCl that saturates the sensing site of this mechanism. However, the TGF-like activity elicits a vasodilator response to a rise in NaCl (38, 44), so that one would have to postulate a reduction in luminal NaCl concentration at the connecting tubule in response to a step increase in RAP to explain the vasoconstriction caused by the third mechanism. Another explanation for the third mechanism might be local ANG II concentration, since a slow regulatory component present at lower RAP was inhibited by AT1 receptor antagonism (8). On the other hand, within the autoregulatory pressure range, ANG II does not seem to have a major impact on steady-state autoregulation (1) or autoregulatory dynamics (23). Furthermore, for ANG II to play an autoregulatory role, one would have to predict that its local concentration gradually increases after a step increase in RAP, which is directionally opposite to the known response of pressure-dependent renin release. A less likely cause of the third mechanism is a progressive decline in proximal tubular reabsorption during a rise in RAP (34). This would augment the load of tubular fluid entering the loop of Henle and could thus increase the error signal perceived by TGF (36). Since this adaptation occurs gradually over the course of >5 min (6), it might contribute to the third mechanism. However, since it should depend on classical TGF, our observed independence from A1AR seems to exclude this possibility. Although the susceptibility to furosemide points toward a tubular cause for the third mechanism, an explanation intrinsic to vascular smooth muscle cannot be entirely dismissed. Since NKCC1, another isoform of the furosemide-sensitive transporter, is expressed on smooth muscle cells and can affect vascular function in vitro (41, 56), an explanation depending on vascular NKCC1 would be compatible with our observation. However, since in our setting MR is enhanced (Fig. 4) rather than attenuated by furosemide (41, 56), it seems unlikely that the concentrations of furosemide reached at the smooth muscle are as high as those in the furosemide-accumulating tubular fluid. It should also be noted that in vivo, furosemide does not induce a dilator response but if anything a reduction of RBF in rats, and this action is unaffected by the presence or absence of NKCC1 (41).

Potential Causes for the Fourth Regulatory Mechanism

If not reflecting a remnant TGF, the fourth mechanism may be mediated by nitric oxide (NO), as this component is reduced by NO synthase inhibition in rats (21). However, clamping of NO levels had little impact on furosemide-resistant autoregulation in dogs (22). A TGF-like activity of the connecting tubule may account for the fourth mechanism, although the response time would be expected to be at least slightly longer than that of classical TGF due to the additional travel time of

the tubular fluid, and one would have to postulate a reduction of tubular NaCl concentrations to explain the observed constrictor response to a rise in RAP. P2X1R-mediated TGF can be ruled out as the underlying cause for the fourth mechanism as it should be eliminated by furosemide (18). Pressure-dependent modulation in proximal tubular reabsorption would seem too slow for the fourth mechanism and due to its inherent involvement of classical TGF should also be inhibited by furosemide. Another possibility is a slow component of MR. However, observations of MR in vascular preparations without TGF present or functional do not support the presence of a biphasic constrictor response of MR (7, 12, 21, 30) other than a rate-sensitive initial overshoot (13, 19). Nevertheless, pressure-dependent modulatory influences on MR in intact tissue but not in isolated vessels remain a possibility.

Relative Contribution of the Autoregulatory Mechanisms

Time windows for RBF autoregulation by MR, TGF/fourth mechanism, and third mechanism were chosen based on the time course of autoregulation during control conditions and furosemide. The autoregulatory strength provided within each of these time windows was found to be 40, 44, and 32%. The overall autoregulatory effort also includes the change in RVR necessary to overcome the initial paradoxical reduction of RVR during step increase of RAP and initial increase in RVR during step reduction. Such initial changes have also been observed by other authors (7, 58) and most likely reflect passive distension and collapse of the resistance vessels by the change in intravascular pressure (12, 30). Because the autoregulation overcoming this distension is afforded in the time window of MR and occurs at a similar rate as the remainder of the autoregulation in the first 5 s, it is ascribed to MR. When the observed autoregulatory strengths are considered in relation to this total autoregulatory action from the initial change to the final level, they correspond to relative contributions of 35, 37, and 28%. Given that TGF and fourth mechanism seem to contribute equally to the second time window, the relative contributions of MR, TGF, third, and fourth mechanism are estimated as 35, 18, 29, and 18%, respectively. This is similar to our findings in rats (20, 21). Based on the data for control conditions from the latter two studies ($n = 51$), the same calculations yield relative contributions of the mechanisms of 41, 22, 15, and 22%. This comparison suggests that the third mechanism in mice seems to have slightly more and MR slightly less influence than in rats, while TGF and fourth mechanism contribute about the same in both species. However, these estimates depend on the assignment of the time windows to specific mechanisms. The assignment of MR and TGF is based on previous literature as explained above. The novel third mechanism is assigned the time window beyond 30 s which is slower than what has been described for the kinetics of classical TGF (3, 10, 15, 28). The third mechanism may start at or even before 5 s after the pressure step. In that case, it would also contribute to the time window assigned to TGF and fourth mechanism. Hence, the contributions based on our current assignments may underestimate the contribution of the third mechanism and overestimate those of TGF and putative fourth mechanism.

Interactions Between TGF and MR Are Not Mediated by A1AR

Furosemide enhances the autoregulatory adjustment due to MR in mice (Fig. 4) as it does in dogs (22) and rats (20, 21). This indicates an interaction between TGF and MR. Such an interaction has also been shown by different methods such as micropuncture (45) and mathematical analysis (5, 37, 42). However, our present results show that ablation of TGF by A1AR deficiency does not affect the strength of MR. Furthermore, the augmenting effect of furosemide on MR is the same whether A1AR are present or not. This implies that despite the obvious importance of A1AR for the vasoconstrictor response of classical TGF, the interaction between TGF and MR is neither mediated nor otherwise modulated by this signaling cascade. Although this may seem counterintuitive, it should be appreciated that furosemide inhibits TGF at the macula densa sensor site, whereas ablation of A1AR interferes with the effector site at the level of the afferent arteriole thereby leaving macula densa function intact. Since stimulation of macula densa cells by elevated luminal NaCl concentration is known to be associated also with release of ATP, NO, and superoxide and with inhibition of PGE_2 production (27, 29), there are multiple potential candidates for mediating the interaction between TGF and MR independent of A1AR. A particularly interesting possibility is NO because it has recently been shown that inhibition of NO synthase (NOS) augments the autoregulatory strength of MR in the kidney through an effect requiring TGF, as it was inhibited by furosemide, did not occur in the TGF-independent hindlimb circulation, and was mimicked by inhibition of only the neuronal isoform of NOS expressed in the macula densa (21, 49). Another possibility is ANG II. It is well-known that a reduced tubular NaCl concentration stimulates renin release, which is mimicked by furosemide (54) and, in contrast to inhibition of renin release by higher NaCl levels, is independent of A1AR (25, 48). Although infusion of ANG II did not affect MR in the intact kidney (21, 23), ANG II was found to enhance MR in kidneys without functional TGF (26). The present finding of independence of the interaction from A1AR places new emphasis on the possible involvement of NO and ANG II in the interaction between TGF and MR stimulating further investigation.

Summary

We conclude that two novel regulatory mechanisms participate in RBF autoregulation in addition to traditional MR and classical TGF. A third mechanism is slower than MR and TGF and independent of A1AR, but it is sensitive to furosemide. The fourth mechanism has kinetics similar to classical TGF but independent of both A1AR and the actions of furosemide. Traditional MR, classical TGF, third, and fourth mechanism contribute 35, 18, 29, and 18% to the overall autoregulatory response in mice. Similar contributions seem to exist in rats. A1AR contribute to autoregulation by mediating classical TGF, the furosemide-sensitive autoregulatory component between 5 and 25 s. In contrast, interaction between TGF and MR is independent of A1AR.

ACKNOWLEDGMENTS

The mice were generously provided and genotyped by Dr. J. B. Schnermann [National Institutes of Health (NIH)-National Institute of Diabetes and Digestive and Kidney Diseases].

GRANTS

The work was supported by NIH Research Grant HL-02334 from the Heart, Blood and Lung Institute, by the Arthur C. Guyton Award for Excellence in Integrative Physiology, and by a gift from the Thomas H. Maren Foundation.

REFERENCES

1. **Arendshorst WJ, Brannstrom K, Ruan X.** Actions of angiotensin II on the renal microvasculature. *J Am Soc Nephrol* 10, *Suppl* 11: S149–S161, 1999.
2. **Arendshorst WJ, Navar LG.** Renal circulation and glomerular hemodynamics. In: *Diseases of the Kidney and Urinary Tract*, edited by Schrier RW. Philadelphia, PA: Lippincott Williams & Wilkins, 2006, p. 59–107.
3. **Bell PD, Thomas C, Williams RH, Navar LG.** Filtration rate and stop-flow pressure feedback responses to nephron perfusion in the dog. *Am J Physiol Renal Fluid Electrolyte Physiol* 234: F154–F165, 1978.
4. **Brown R, Ollerstam A, Johansson B, Skott O, Gebre-Medhin S, Fredholm B, Persson AE.** Abolished tubuloglomerular feedback and increased plasma renin in adenosine A(1) receptor-deficient mice. *Am J Physiol Regul Integr Comp Physiol* 281: R1362–R1367, 2001.
5. **Chon KH, Chen YM, Marmarelis VZ, Marsh DJ, Holstein-Rathlou NH.** Detection of interactions between myogenic and TGF mechanisms using nonlinear analysis. *Am J Physiol Renal Fluid Electrolyte Physiol* 267: F160–F173, 1994.
6. **Chou CL, Marsh DJ.** Time course of proximal tubule response to acute arterial hypertension in the rat. *Am J Physiol Renal Fluid Electrolyte Physiol* 254: F601–F607, 1988.
7. **Clausen G, Oien AH, Aukland K.** Myogenic vasoconstriction in the rat kidney elicited by reducing perirenal pressure. *Acta Physiol Scand* 144: 277–290, 1992.
8. **Cupples WA.** Angiotensin II conditions the slow component of autoregulation of renal blood flow. *Am J Physiol Renal Fluid Electrolyte Physiol* 264: F515–F522, 1993.
9. **Cupples WA, Novak P, Novac V, Salevsky FC.** Spontaneous blood pressure fluctuations and renal blood flow dynamics. *Am J Physiol Renal Fluid Electrolyte Physiol* 270: F82–F89, 1996.
10. **Daniels FH, Arendshorst WJ.** Tubuloglomerular feedback kinetics in spontaneously hypertensive and Wistar-Kyoto rats. *Am J Physiol Renal Fluid Electrolyte Physiol* 259: F529–F534, 1990.
11. **Daniels FH, Arendshorst WJ, Roberds RG.** Tubuloglomerular feedback and autoregulation in spontaneously hypertensive rats. *Am J Physiol Renal Fluid Electrolyte Physiol* 258: F1479–F1489, 1990.
12. **Davis MJ, Sikes PJ.** Myogenic responses of isolated arterioles: test for a rate-sensitive mechanism. *Am J Physiol Heart Circ Physiol* 259: H1890–H1900, 1990.
13. **Grande PO.** Dynamic and static components in the myogenic control of vascular tone in cat skeletal muscle. *Acta Physiol Scand Suppl* 476: 1–44, 1979.
14. **Hashimoto S, Huang Y, Briggs J, Schnermann J.** Reduced autoregulatory effectiveness in adenosine 1 receptor-deficient mice. *Am J Physiol Renal Physiol* 290: F888–F891, 2006.
15. **Holstein-Rathlou NH, Marsh DJ.** Oscillations of tubular pressure, flow, and distal chloride concentration in rats. *Am J Physiol Renal Fluid Electrolyte Physiol* 256: F1007–F1014, 1989.
16. **Holstein-Rathlou NH, Wagner AJ, Marsh DJ.** Tubuloglomerular feedback dynamics and renal blood flow autoregulation in rats. *Am J Physiol Renal Fluid Electrolyte Physiol* 260: F53–F68, 1991.
17. **Inscho EW, Cook AK, Imig JD, Vial C, Evans RJ.** Renal autoregulation in P2X1 knockout mice. *Acta Physiol Scand* 181: 445–453, 2004.
18. **Inscho EW, Cook AK, Imig JD, Vial C, Evans RJ.** Physiological role for P2X1 receptors in renal microvascular autoregulatory behavior. *J Clin Invest* 112: 1895–1905, 2003.
19. **Johansson B, Mellander S.** Static and dynamic components in the vascular myogenic response to passive changes in length as revealed by electrical and mechanical recordings from the rat portal vein. *Circ Res* 36: 76–83, 1975.
20. **Just A, Arendshorst WJ.** Dynamics and contribution of mechanisms mediating renal blood flow autoregulation. *Am J Physiol Regul Integr Comp Physiol* 285: R619–R631, 2003.
21. **Just A, Arendshorst WJ.** Nitric oxide blunts myogenic autoregulation in rat renal but not skeletal muscle circulation via tubuloglomerular feedback. *J Physiol* 569: 959–974, 2005.
22. **Just A, Ehmke H, Toktomambetova L, Kirchheim HR.** Dynamic characteristics and underlying mechanisms of renal blood flow autoregulation in the conscious dog. *Am J Physiol Renal Physiol* 280: F1062–F1071, 2001.
23. **Just A, Ehmke H, Wittmann U, Kirchheim HR.** Role of angiotensin II in dynamic renal blood flow autoregulation of the conscious dog. *J Physiol* 538: 167–177, 2002.
24. **Just A, Wittmann U, Ehmke H, Kirchheim HR.** Autoregulation of renal blood flow in the conscious dog and the contribution of the tubuloglomerular feedback. *J Physiol* 506: 275–290, 1998.
25. **Kim SM, Mizel D, Huang YG, Briggs JP, Schnermann J.** Adenosine as a mediator of macula densa-dependent inhibition of renin secretion. *Am J Physiol Renal Physiol* 290: F1016–F1023, 2006.
26. **Kirton CA, Loutzenhiser R.** Alterations in basal protein kinase C activity modulate renal afferent arteriolar myogenic reactivity. *Am J Physiol Heart Circ Physiol* 275: H467–H475, 1998.
27. **Komlosi P, Fintha A, Bell PD.** Current mechanisms of macula densa cell signalling. *Acta Physiol Scand* 181: 463–469, 2004.
28. **Leyssac PP, Baumbach L.** An oscillating intratubular pressure response to alterations in Henle loop flow in the rat kidney. *Acta Physiol Scand* 117: 415–419, 1983.
29. **Liu R, Garvin JL, Ren Y, Pagano PJ, Carretero OA.** Depolarization of the macula densa induces superoxide production via NAD(P)H oxidase. *Am J Physiol Renal Physiol* 292: F1867–F1872, 2007.
30. **Loutzenhiser R, Bidani A, Chilton L.** Renal myogenic response: kinetic attributes and physiological role. *Circ Res* 90: 1316–1324, 2002.
31. **Majid DS, Inscho EW, Navar LG.** P2 purinoceptor saturation by adenosine triphosphate impairs renal autoregulation in dogs. *J Am Soc Nephrol* 10: 492–498, 1999.
32. **Marsh DJ, Sosnovtseva OV, Chon KH, Holstein-Rathlou NH.** Nonlinear interactions in renal blood flow regulation. *Am J Physiol Regul Integr Comp Physiol* 288: R1143–R1159, 2005.
33. **Mattson DL.** Long-term measurement of arterial blood pressure in conscious mice. *Am J Physiol Regul Integr Comp Physiol* 274: R564–R570, 1998.
34. **McDonough AA, Leong PK, Yang LE.** Mechanisms of pressure natriuresis: how blood pressure regulates renal sodium transport. *Ann NY Acad Sci* 986: 669–677, 2003.
35. **Mitchell KD, Navar LG.** Modulation of tubuloglomerular feedback responsiveness by extracellular ATP. *Am J Physiol Renal Fluid Electrolyte Physiol* 264: F458–F466, 1993.
36. **Moore LC.** Interaction of tubuloglomerular feedback and proximal nephron reabsorption in autoregulation. *Kidney Int Suppl* 12: S173–S178, 1982.
37. **Moore LC, Rich A, Casellas D.** Ascending myogenic autoregulation: interactions between tubuloglomerular feedback and myogenic mechanisms. *Bull Math Biol* 56: 391–410, 1994.
38. **Morsing P, Velazquez H, Ellison D, Wright FS.** Resetting of tubuloglomerular feedback by interrupting early distal flow. *Acta Physiol Scand* 148: 63–68, 1993.
39. **Navar LG, Inscho EW, Majid DSA, Imig JD, Harrison Bernard LM, Mitchell KD.** Paracrine regulation of the renal microcirculation. *Physiol Rev* 76: 425–536, 1996.
40. **Nishiyama A, Jackson KE, Majid DS, Rahman M, Navar LG.** Renal interstitial fluid ATP responses to arterial pressure and tubuloglomerular feedback activation during calcium channel blockade. *Am J Physiol Heart Circ Physiol* 290: H772–H777, 2006.
41. **Oppermann M, Hansen PB, Castrop H, Schnermann JB.** Vasodilatation of afferent arterioles and paradoxical increase of renal vascular resistance by furosemide in mice. *Am J Physiol Renal Physiol* 293: F279–F287, 2007.
42. **Raghavan R, Chen X, Yip KP, Marsh DJ, Chon KH.** Interactions between TGF-dependent and myogenic oscillations in tubular pressure and whole kidney blood flow in both SDR and SHR. *Am J Physiol Renal Physiol* 290: F720–F732, 2006.
43. **Ren Y, Garvin JL, Liu R, Carretero OA.** Role of macula densa adenosine triphosphate (ATP) in tubuloglomerular feedback. *Kidney Int* 66: 1479–1485, 2004.

44. **Ren Y, Garvin JL, Liu R, Carretero OA.** Crosstalk between the connecting tubule and the afferent arteriole regulates renal microcirculation. *Kidney Int* 71: 1116–1121, 2007.
45. **Schnermann J, Briggs JP.** Interaction between loop of Henle flow and arterial pressure as determinants of glomerular pressure. *Am J Physiol Renal Fluid Electrolyte Physiol* 256: F421–F429, 1989.
46. **Schnermann J, Levine DZ.** Paracrine factors in tubuloglomerular feedback: adenosine, ATP, and nitric oxide. *Annu Rev Physiol* 65: 501–529, 2003.
47. **Schnermann J, Weihprecht H, Briggs JP.** Inhibition of tubuloglomerular feedback during adenosine 1 receptor blockade. *Am J Physiol Renal Fluid Electrolyte Physiol* 258: F553–F561, 1990.
48. **Schweda F, Segerer F, Castrop H, Schnermann J, Kurtz A.** Blood pressure-dependent inhibition of Renin secretion requires A1 adenosine receptors. *Hypertension* 46: 780–786, 2005.
49. **Shi Y, Wang X, Chon KH, Cupples WA.** Tubuloglomerular feedback-dependent modulation of renal myogenic autoregulation by nitric oxide. *Am J Physiol Regul Integr Comp Physiol* 290: R982–R991, 2006.
50. **Siu KL, Chon KH, Sung B, Birzgalis A, Moore LC.** Modulation of autoregulatory mechanisms by very-low frequency (VLF) rhythms in RBF (Abstract). *FASEB J* 20: A761, 2006.
51. **Sosnovtseva OV, Pavlov AN, Mosekilde E, Holstein-Rathlou NH, Marsh DJ.** Double-wavelet approach to studying the modulation properties of non-stationary multimode dynamics. *Physiol Meas* 26: 351–362, 2005.
52. **Sun D, Samuelson LC, Yang T, Huang Y, Paliege A, Saunders T, Briggs J, Schnermann J.** Mediation of tubuloglomerular feedback by adenosine: evidence from mice lacking adenosine 1 receptors. *Proc Natl Acad Sci USA* 98: 9983–9988, 2001.
53. **Thomson S, Bao D, Deng A, Vallon V.** Adenosine formed by 5′-nucleotidase mediates tubuloglomerular feedback. *J Clin Invest* 106: 289–298, 2000.
54. **Vander AJ.** Control of renin release. *Physiol Rev* 47: 359–382, 1967.
55. **Walker M III, Harrison-Bernard LM, Cook AK, Navar LG.** Dynamic interaction between myogenic and TGF mechanisms in afferent arteriolar blood flow autoregulation. *Am J Physiol Renal Physiol* 279: F858–F865, 2000.
56. **Wang X, Breaks J, Loutzenhiser K, Loutzenhiser R.** Effects of inhibition of the $Na^+/K^+/2Cl^-$ cotransporter on myogenic and angiotensin II responses of the rat afferent arteriole. *Am J Physiol Renal Physiol* 292: F999–F1006, 2007.
57. **Wronski T, Seeliger E, Persson PB, Forner C, Fichtner C, Scheller J, Flemming B.** The step response: a method to characterize mechanisms of renal blood flow autoregulation. *Am J Physiol Renal Physiol* 285: F758–F764, 2003.
58. **Young DK, Marsh DJ.** Pulse wave propagation in rat renal tubules: implications for GFR autoregulation. *Am J Physiol Renal Fluid Electrolyte Physiol* 240: F446–F458, 1981.